# Introducing compression platen misalignment in single fiber transverse compression analytical models

Jason Govilas[1], Violaine Guicheret-Retel[2], Cédric Clévy[1], Vincent Placet[1] and Fabien Amiot[1*]

[1*]Université de Franche-Comté, CNRS, institut FEMTO-ST, 24 chemin de l'Épitaphe, Besançon, 25030, France.
[2*]SUPMICROTECH, CNRS, institut FEMTO-ST, 26 chemin de l'Épitaphe, Besançon, 25030, France.

**Abstract**

Analytical models of Single Fiber Transverse Compression Tests (SFTCTs) are commonplace for the identification of a fiber's apparent transverse elastic modulus $\boldsymbol{E_T}$ by inverse method. Compression platen misalignment however, has been shown to induce important identification errors due to the change in the platen-fiber contact surface compared to the parallel platen configuration. Nevertheless, methods to minimize this misalignment experimentally are sparse in the literature and no existing analytical models take it into consideration. In this paper the development of such a model is presented, which accounts for the angle around the fiber's pitch axis, named "tilt" angle. The predictions of this analytical model are shown to closely match the results of an equivalent Finite Element Model (FEM). Using force and displacement data resulting from this Finite Element Analysis (FEA), along with fiber's material and geometric properties and the value of the tilt angle, the proposed analytical model produces very low identification errors of $\boldsymbol{E_T}$, independently of the tilt angle. The proposed model can thus be used to reliably identify a fiber's transverse elastic modulus even for SFTCTs where a tilt angle is present.

**Keywords:** compression test, fiber mechanical characterization, parallelism error, extended Jawad-Ward model

# 1 Introduction

Fibers are a widely used structural and functional material in a wide variety of applications ranging from textiles and composites to energy harvesting, temperature regulation, biomedical use and more [1]. Fibers can be natural (plant, animal, mineral) or man-made (carbon, polymer, aramide...) providing different properties and sustainability benefits depending on their source [1–3]. Knowledge of the transverse mechanical properties of these fibers is key in modeling and predicting the behavior of the structures that incorporate them or in cases where fibers are subject to important transverse loads such as ballistic impacts [4], composite material compression molding [5] or plant fiber extraction [3].

To characterize fiber transverse mechanical properties, Single Fiber Transverse Compression Tests (SFTCTs) represent the established direct testing method. The test consists of compressing a unitary fiber between two compression platens, one of them being fixed and the other mobile. Analytical models predict, through various formulations, the fiber's behavior under this transverse compression. The origins of all SFTCT models can be traced to Hertz's contact theory [6] and more specifically McEwen's [7] formulation of contact stresses in parallel elastic cylinders under transverse compression. Based on these works Hadley et al. [8] proposed a formulation to calculate the contact half-width $b$, in the context of single fiber transverse compression. Morris [9], Phoenix et al. [10], Jawad et al. [11] and Cheng et al. [12] incorporated Hadley's formulation of the contact half-width and iterated on models that offer the

fiber's radial displacement, as a function of the applied compressive force and the fiber's geometric and material properties.

In all these aforementioned analytical models, the fiber's geometry is approximated to a right circular cylinder. Since a fiber's length is significantly larger than its diameter, the problem is formulated in plane strain conditions, omitting the fiber's longitudinal strain. An infinitesimal strain approach is used. While fibers can exhibit complex inelastic behavior, isotropic or transversely isotropic elastic behavior hypotheses are used in these models. With the use of these models, an apparent transverse elastic modulus $E_T$ of the fiber can be identified by inverse method by performing SFTCTs.

Analytical models of SFTCTs also make hypotheses that are not inherent to fiber nature. Since the compression platens are made from materials (typically sapphire, glass) that are significantly stiffer than the fiber, they are considered as rigid. Furthermore, the two compression platens are considered as perfectly parallel. In practice however, assuring this parallelism experimentally can prove challenging. Failing to find any mention of parallelism control in the SFTCT literature is not a rare occurrence. Our team has demonstrated that platen misalignment can have a major influence on the fiber's identified apparent transverse elastic modulus [18]. The study was focused on the rotation of the upper compression platen around the fiber's pitch axis, as seen in Fig 1. The angle associated to this rotation around the $x$ axis was termed "tilt angle" and noted $\phi$. The tilt angle produces the largest variation of the contact surface between the platen and the fiber, resulting in a large error in the identification of $E_T$, with an angle of 1° leading to an identification error of around 90%. An experimental protocol was proposed to minimize the tilt angle under 0.1°, however a custom force-displacement sensor and precise actuation were required to achieve it. Other methods of minimizing platen misalignment

in SFTCTs have been proposed in the literature such as manual adjustments [8], passive alignment methods [13, 14], platen preloading [15, 16] and active motors [17], however no quantification of the platen parallelism accuracy was provided in these studies.

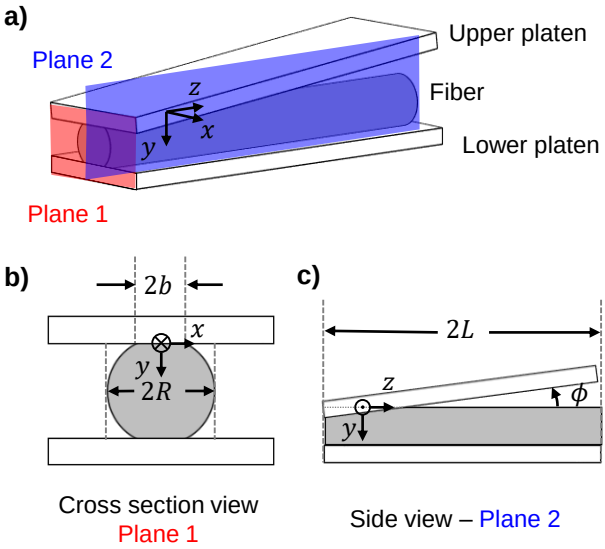


**Fig. 1** a) Representation of a single fiber transverse compression test with a tilt angle $\phi$, b) cross section view with the fiber with a contact width of $2b$, c) side view of SFTCT with a tilt angle. The origin of the reference system is placed, along the $z$ axis, on the center of zone of the fiber that is in contact with the upper platen.

An alternative-complementary approach to an active correction of the tilt angle before SFTCTs lies in introducing it directly in the analytical model of the test. This would allow a better identification of $E_T$ when a small tilt angle persists after parallelism setting procedures, or even potentially eliminate the need for such procedures and the related equipment altogether. Resources and time constraints related to platen parallelism control could thus be significantly reduced. In this paper, such a SFTCT model is developed by extending the model developed by Jawad and Ward [11], to account for the presence of a tilt angle (*i.e.,* a rotation of the upper platen around the $x$ axis). To facilitate

comparisons the term "tilt model" is used to refer to the newly developed model while "Jawad-Ward model" is used for the original formulation. A Finite Element Model (FEM) of a SFTCT performed with a tilt angle is used to validate the predictions of the tilt model and compare its identification error with the Jawad-Ward model.

## 2 SFTCT analytical model tilt angle extension

In this section the development of the analytical model that accounts for the presence of a tilt angle in SFTCTs is presented. The widely used model developed by Jawad and Ward [11] serves as basis in this development and is extented to incorporate the tilt angle. Its original formulation provides the radial displacement of a fiber, represented as a right circular cylinder, under compression between two parallel and rigid compression platens with:

$$U = \frac{4F_L}{\pi}\left\{\alpha_1\Big(sinh^{-1}(R/b) + ln(2)\Big) - \frac{1}{2}(\alpha_1 + \alpha_2) + \alpha_2\frac{R}{b}\left(\sqrt{1+(R/b)^2} - R/b\right)\right\} \quad (1)$$

with: $F_L$ the compressive force per unit of length, $U$ the fiber's radial displacement along the $y$ axis and $R$ the fiber's radius (see Fig. 1). The term $b$ corresponds to the half contact width given by:

$$b = \sqrt{\frac{4F_L R}{\pi}\alpha_1} \quad (2)$$

The model represents the fiber as transversely isotropic with the fiber's logitudinal axis ($z$ axis), being the axis of symmetry. The terms $\alpha_1$ and $\alpha_2$ relate

the fiber's material properties to the rest of the model through:

$$\alpha_1 = \frac{1}{E_T} - \frac{\nu_{LT}^2}{E_L} \tag{3}$$

$$\alpha_2 = -\frac{\nu_{TT}}{E_T} - \frac{\nu_{LT}^2}{E_L} \tag{4}$$

with: $E_T$ the fiber's transverse elastic modulus, $E_L$ the longitudinal modulus and $\nu_{LT}$ and $\nu_{TT}$ the Poisson ratios in the longitudinal and transverse plane respectively.

The first step in development of an extended model that accounts for the tilt angle consists in the nondimensionalization of the initial equation :

$$\tilde{U} = \tilde{b}^2 \left\{ \sinh^{-1}\left(\tilde{b}^{-1}\right) + \ln 2 - \frac{1}{2}\left(1 + \frac{\alpha_2}{\alpha_1}\right) + \frac{\alpha_2}{\alpha_1}\tilde{b}^{-1}\left(\sqrt{1+\tilde{b}^{-2}} - \tilde{b}^{-1}\right) \right\} \tag{5}$$

where:

$$\tilde{U} = \frac{U}{R} \tag{6}$$

$$\tilde{b} = \frac{b}{R} \tag{7}$$

Assuming that $\tilde{b}$ is small enough, Eq. 5 may be approached by a Taylor expansion:

$$\begin{aligned} \tilde{U} = & -\tilde{b}^2 \ln\left(\tilde{b}\right) + \sum_{k=1}^{\infty} (-1)^{k+1} \frac{(2k)!\,\tilde{b}^{2(k+1)}}{2^{2k}(k!)^2 2k} \\ & + \left(2\ln 2 - \frac{1}{2}\left(1 + \frac{\alpha_2}{\alpha_1}\right)\right)\tilde{b}^2 \\ & + \frac{\alpha_2}{2\alpha_1}\left(\tilde{b}^2 + \sum_{k=2}^{\infty} (-1)^{k+1} \frac{\prod_{p=0}^{k-2}(2p+1)}{2^{k-1}k!}\tilde{b}^{2k}\right) \end{aligned} \tag{8}$$

One assumes that the plates are much stiffer than the tested fiber, so that the tilt angle $\phi$ results in a linear compression of the fiber. Considering that the origin of the reference frame is placed, along the $z$ axis, at the center of the contact zone between the fiber and the upper platen, as seen in Fig 1, the following stands:

$$\tilde{U}(z) = \frac{U(z=0) - z\tan\phi}{R} = \tilde{U_0} - \frac{z}{R}\tan\phi \tag{9}$$

where:

$$\tilde{U_0} = \frac{U(z=0)}{R} \tag{10}$$

The contact width field $b(z)$ resulting from the linear compression field defined by Eq. (9) is now sought. Let us denote $\tilde{b_0}$ the value such that:

$$\begin{aligned}\tilde{U_0} \;=\; \tilde{b_0}^{\,2}\Bigg\{&\sinh^{-1}\left(\tilde{b_0}^{\,-1}\right) + \ln 2 - \frac{1}{2}\left(1 + \frac{\alpha_2}{\alpha_1}\right) \\ &+ \frac{\alpha_2}{\alpha_1}\tilde{b_0}^{\,-1}\left(\sqrt{1+\tilde{b_0}^{\,-2}} - \tilde{b_0}^{\,-1}\right)\Bigg\}\end{aligned} \tag{11}$$

The field $\tilde{b}(z)$ is sought as:

$$\tilde{b}(z) = \sum_{k=0}^{\infty}\tilde{b_k}z^k = \tilde{b_0}\left(1 + \sum_{k=1}^{\infty}\frac{\tilde{b_k}}{\tilde{b_0}}z^k\right) = \tilde{b_0}\left(1 + \sum_{k=1}^{\infty}\hat{b_k}z^k\right) \tag{12}$$

where:

$$\hat{b_k} = \frac{\tilde{b_k}}{\tilde{b_0}} \tag{13}$$

The terms involved in Eq. (8) thus read:

$$\ln\tilde{b} \;=\; \ln\tilde{b_0} + \sum_{k=1}^{\infty} c_k z^k \tag{14}$$

$$\tilde{b}^n = \sum_{k=0}^{\infty} d_k z^k \tag{15}$$

where $c_k$ are obtained using (0.315) in [19]:

$$\begin{aligned} c_1 &= \hat{b_1} \\ c_2 &= \hat{b_2} - \frac{\hat{b_1}^2}{2} \\ c_3 &= \hat{b_3} - \hat{b_1}\hat{b_2} + \frac{\hat{b_1}^3}{3} \\ &\text{etc...} \end{aligned} \tag{16}$$

and the $d_k$ are obtained recursively using (0.314) in [19]:

$$\begin{aligned} d_0 &= \tilde{b_0}^n \\ d_m &= \frac{1}{m\tilde{b_0}} \sum_{k=1}^{m} (kn - m + k)\tilde{b_k} d_{m-k} \quad \text{for } m \geq 1 \end{aligned} \tag{17}$$

Ones assumes that Eq. (5), which has been derived for plane strain, holds locally. Keeping the Taylor expansion (8) up to the second order (which is a very good approximation up to $\frac{b}{R} \simeq 0.4$ for any values of the material parameters), the normalized compression field therefore reads:

$$\begin{aligned} \tilde{U}(z) \simeq \tilde{U}_0 \\ &+z\left(-\tilde{b_0}^2 c_1 - 2\tilde{b_0}\tilde{b_1}\ln\tilde{b_0} + 2\left(2\ln 2 - \frac{1}{2}\right)\tilde{b_0}\tilde{b_1}\right) \\ &+z^2\left(-\tilde{b_0}^2 c_2 - 2\tilde{b_0}\tilde{b_1}c_1 - \left(\tilde{b_1}^2 + 2\tilde{b_2}\tilde{b_0}\right)\ln\tilde{b_0}\right. \\ &\qquad \left. + \left(2\ln 2 - \frac{1}{2}\right)\left(\tilde{b_1}^2 + 2\tilde{b_2}\tilde{b_0}\right)\right) \\ &+z^3\left(-\tilde{b_0}^2 c_3 - 2\tilde{b_0}\tilde{b_1}c_2 - \left(\tilde{b_1}^2 + 2\tilde{b_2}\tilde{b_0}\right)c_1 - 2\left(\tilde{b_1}\tilde{b_2} + \tilde{b_0}\tilde{b_3}\right)\ln\tilde{b_0}\right. \\ &\qquad \left. +2\left(2\ln 2 - \frac{1}{2}\right)\left(\tilde{b_1}\tilde{b_2} + \tilde{b_0}\tilde{b_3}\right)\right) \end{aligned}$$

$$+\dots \tag{18}$$

Comparing Eqs (9) and (18) directly yields the linear system to be solved:

$$\begin{aligned}
-\frac{\tan\phi}{R} &= -\tilde{b_0}^2 c_1 - 2\tilde{b_0}\tilde{b_1}\ln\tilde{b_0} + 2\left(2\ln 2 - \frac{1}{2}\right)\tilde{b_0}\tilde{b_1} \\
0 &= -\tilde{b_0}^2 c_2 - 2\tilde{b_0}\tilde{b_1}c_1 - \left(\tilde{b_1}^2 + 2\tilde{b_2}\tilde{b_0}\right)\ln\tilde{b_0} + \left(2\ln 2 - \frac{1}{2}\right)\left(\tilde{b_1}^2 + 2\tilde{b_2}\tilde{b_0}\right) \\
0 &= -\tilde{b_0}^2 c_3 - 2\tilde{b_0}\tilde{b_1}c_2 - \left(\tilde{b_1}^2 + 2\tilde{b_2}\tilde{b_0}\right)c_1 - 2\left(\tilde{b_1}\tilde{b_2} + \tilde{b_0}\tilde{b_3}\right)\ln\tilde{b_0} \\
&\quad +2\left(2\ln 2 - \frac{1}{2}\right)\left(\tilde{b_1}\tilde{b_2} + \tilde{b_0}\tilde{b_3}\right) \\
&\dots
\end{aligned} \tag{19}$$

The system is easily solved sequentially with $\tilde{b_0}$ being found through Eq.(11): the first equation of the system yields $\tilde{b_1}$, the second subsequently yields $\tilde{b_2}$ and so on. The proposed sequence is therefore easily coded to yield all the desired $\tilde{b_k}$ and thus, assuming convergence, the function $\tilde{b}(z)$. It is worth noting that the proposed correction does not depend on the fiber's elastic properties. From Eq. (2), the force per unit of length as a function of $z$ can also be expressed:

$$F_L(z) = \frac{\pi b^2(z)}{4\alpha_1 R} \tag{20}$$

The force per unit of length may be integrated over the contact length $\mathcal{L}$ to yield the net force $F$ applied to the fiber:

$$F = \int_{\mathcal{L}} F_L(z)dz \tag{21}$$

In conclusion, the net force applied to the fiber $F$, can be calculated, for any tilt angle, with the fiber's displacement at $z = 0$ ($U(z = 0)$) and the rest

of its geometric and material properties as an input. Using an inverse method, the fiber's transverse elastic modulus $E_T$ can be identified if force-displacement data along with the tilt angle and the fiber's properties are provided.

# 3 Materials and Methods

## 3.1 Finite element model

In order to validate the newly developed tilt model, its predictions are compared to those of a FEM. A model developed by our team in COMSOL Multiphysics ® and first presented in [18] is used for this purpose. A brief description of the model is given below. Half of the fiber and the platens are modeled by applying a symmetry condition along the $yz$ plane. The lower platen is fixed while the upper platen is mobile with an imposed displacement of $1\,\mu m$ along the $y$ axis and rotated with tilt angles varying from 0° to 1°. A linear strain formulation is used to better match the infinitesimal strain approach used in the analytical model. The contact between the platen and the fiber is modeled through a Lagrangian formulation. A polyamide 11 (PA11) fiber is modeled as a transversely isotropic right circular cylinder. Its geometric and material properties are given in Table 1.

| Parameter | Values | Description |
|---|---|---|
| R ($\mu$m) | 17.05 | Radius |
| 2L ($\mu$m) | 300 | Compressed length |
| $E_L$ (MPa) | 2155 | Longitudinal Young's modulus |
| $E_T$ (MPa) | 706 | Transverse Young's modulus |
| $\nu_{LT}$ | 0.4 | Poisson's ratio in longitudinal plane |
| $\nu_{TT}$ | 0.07 | Poisson's ratio in transverse plane |
| $G_{LT}$ (MPa) | 1000 | Shear modulus |

**Table 1** PA11 fiber geometric and material properties. Sources and measurements of these parameters are given in [18].

The mesh of the model consists of prisms with triangular cross sections for the fiber and rectangular ones for the platens. Second-order elements are

used. The mesh is slightly adjusted compared to the model presented in [18]. A potential contact zone between the fiber and the upper and lower platen is defined along an arc of 30°, with 14 elements placed along its length. An adjustment of the mesh along the fiber's length is also made, with a ratio of $|1 - 500 \cdot \sin\phi|$ between the length of the first element, situated at the edge of the fiber that is in contact with the upper platen, and the last element on the opposite end of the fiber, which is potentially not in contact with the platen, depending on the tilt angle. In this way, a uniform mesh along the fiber length is obtained when the platens are parallel ($\phi = 0°$) while an active refinement along the contact zone is performed as the tilt increases. The geometry, boundary conditions and mesh of the model are shown in Fig 2.

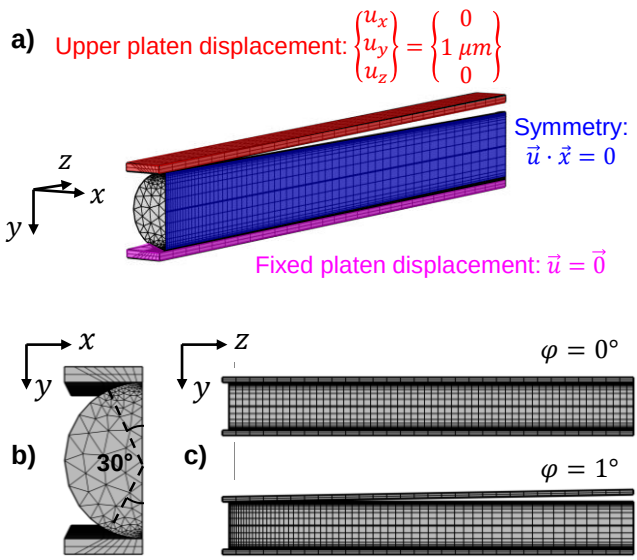


**Fig. 2** Finite element model of SFTCT with an upper platen tilt angle misalignment: a) boundary conditions, b) cross section view of mesh with defined potential contact zones, c) side view of mesh with tilt angle-adaptive mesh.

### 3.2 Transverse elastic modulus identification

In order to validate the developed analytical model, its ability to identify the fiber's transverse elastic modulus $E_T$ by inverse method at different tilt angles is evaluated. To do so, force and displacement data issued from the Finite Element Analysis (FEA) are used. The displacement of the upper platen is taken, which is equivalent to the fiber's vertical displacement at the point where the first contact occurs. The applied compressive force $F$, is evaluated by integrating the $y$ axis component of the contact pressure on the top surface of the fiber where it is in contact with the upper compression platen.

The inverse identification is performed through a trust-region algorithm by providing the compressive force $F$, the upper platen displacement $U$, the tilt angle $\phi$ and the fiber's geometric and material properties ($R$, $E_L$, $\nu_{LT}$, $\nu_{TT}$). Eq. (12) is truncated at orders $k \leq 5$ in the formulation of the tilt model. To evaluate the model's identification ability at different tilt angles, the identified transverse elastic modulus $E_{T_{id}}$ is compared with the one identified for a compression with parallel platens $E_{T_0}$ by calculating their relative difference $\Delta E_T$:

$$\Delta E_T = \frac{E_{T_{id}} - E_{T_0}}{E_{T_0}} \tag{22}$$

The influence of the truncation order in the expression of the field $b(\tilde{z})$ in Eq. (12) is also studied. Specifically, its influence on the identification of $E_T$ is assessed by evaluating $\Delta E_T$ as a function of a truncation order, varied from 1 to 5. A convergence in the value of $E_T$ that is identified by the tilt model can thus be verified.

## 4 Results and discussions

The results of the identification procedure using the Jawad-Ward and tilt model with an expansion order of 5, is shown in Fig. 3. Regarding the

force-displacement results, the typical non-linearity obtained for purely elastic materials under SFTCT can be seen in Fig. 3.a. The tilt model closely matches the FEA results for all tilt angles. On the other hand, the Jawad-Ward model, that does not take into account the tilt angle, only fits the FEA results well for a tilt angle of 0° with important differences appearing for non-zero tilt angles.

These differences are reflected in the values of the identified transverse elastic modulii. As seen in Fig. 3.b, the Jawad-Ward model significantly underestimates the fiber's transverse elastic modulus, as attested by the negative values of $\Delta E_T$, which can reach up to -90% for tilt angles of only 1°. Conversely, the modulii values identified with the tilt model are close to the one identified with parallel platens. Only, a slight increase in $\Delta E_T$ takes place with the increase in angle, that reaches 1.3% for a tilt angle of 1°. Despite this small increase, the model's overall ability to account for the presence of a tilt angle is demonstrated.

It can be noted that for a tilt angle of 0° a relative difference of $-0.6\%$ and $-0.7\%$ between the identified transverse elastic modulus and the one imposed in the simulation exists, for the Jawad-Ward and the tilt model respectively. This small difference can be explained by the presence of longitudinal strains in the 3D SFTCT finite element model, as opposed to the 2D, plane strain analytical models used in the identification, as explained in [18]. The non-uniform loading along the $z$ direction for a tilt angle $\phi \neq 0°$ may also be expected to be at the origin of an additional deviation from the plane strain assumption. The quality of this assumption may be further assessed by analyzing the effect of $G_{LT}$ on the identification error. Varying $G_{LT}$ over almost 10 decades, the identification error is shown to vary by a few percent, thereby proving the negligible sensitivity of the reported results to $G_{LT}$. This further validates the use of plane strain assumption.

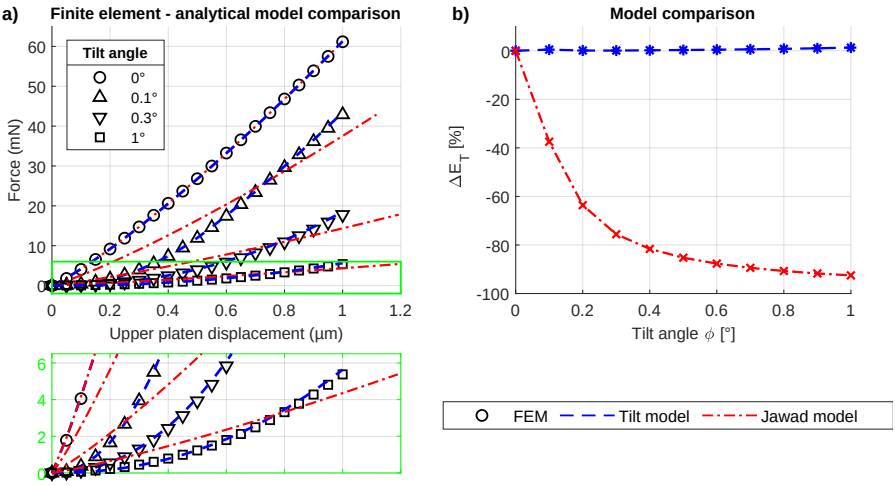


**Fig. 3** Transverse elastic modulus identification results with the use of the Jawad-Ward and tilt model: a) force-displacement FEM results for different tilt angles (markers) with fitted analytical models (dotted lines), b) evolution of $\Delta E_T$ as function of tilt angle for both analytical models.

The impact on $\Delta E_T$ of the truncation order used in Eq. (12) can be seen in Fig. 4. A decrease in $\Delta E_T$ is observed with the increase in expansion order. This decrease is significant when switching from order 1 to 2. For higher orders however, $\Delta E_T$ converges towards values of 1.3%.

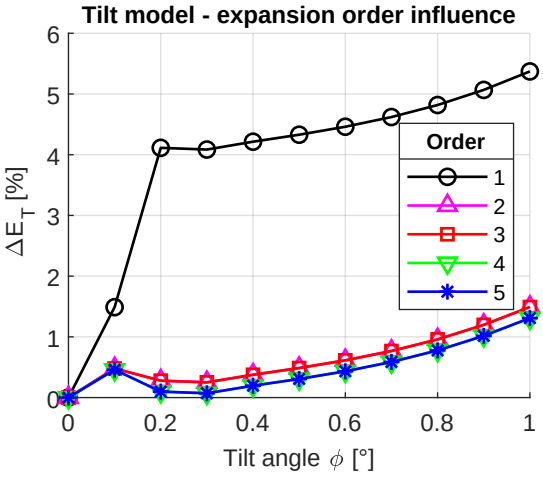


**Fig. 4** Evolution of $\Delta E_T$ as a function of tilt angle for different expansion orders in Eq. (12) of the tilt model.

# 5 Conclusions

Compression platen misalignment represents a significant source of error in the identification of a fiber's transverse elastic modulus through SFTCts. In this paper, an analytical model which accounts for the presence of a tilt angle is developed by extending the model proposed by Jawad and Ward [11]. Using data from a finite element model of a SFTCT with a tilt angle, the proposed "tilt model" is shown to identify the fiber's transverse elastic modulus with an error under 1.5% for all tested tilt angles. The identification of a fiber's transverse elastic modulus $E_T$ can thus be made with very low errors compared to those obtained with the standard model, regardless of the tilt angle. The predictions of the tilt model also closely match the results of the FEA. Modeling SFTCTs with a tilt angle can thus be achieved with the tilt model instead of a 3D FEM, saving development and computation time [20]. Furthermore, the tilt model contributes significantly in reducing experimental constraints on compression platen parallelism in SFTCTs. As long as the tilt angle between compression platens can be measured, with optical means for example, the uncertainty on the identified value of $E_T$ that is related to platen parallelism is significantly reduced. The need for complex or time-consuming parallelism setting procedures and their related equipment could thus be reduced or eliminated.

Further work can be performed to account for platen rotations around the $z$ axis as well. Additionally, the parallel identification of both the transverse elastic modulus and the tilt angle could be considered, eliminating the need for misalignment angle measurements. This parallel identification however requires further data in order to provide reliable results, such as the displacement fields at the fiber's edge. Finally, it can be noted that while the

proposed model is developed in the case of the SFTCT, the underlying principle of its development could be used for the compression of other objects at any scale, providing an alternative to parallelism setting procedures across various mechanical tests and scientific disciplines.

## Acknowledgements

This work has been supported by the EIPHI Graduate School under grant "ANR-17-EURE-0002".

## Conflicts of interest or competing interests

The authors declare no competing interest.

## Data and code availability

An Octave/Matlab implementation of the approach proposed herein is available [20].

## Supplementary information

Not applicable.

## Ethical approval

Not applicable.

## References

[1] Chang H, Luo J, Gulgunje P V., Kumar S (2017) Structural and Functional Fibers. Annu Rev Mater Res 47:331–359. https://doi.org/10.1146/annurev-matsci-120116-114326

[2] Khan T, Hameed Sultan MT Bin, Ariffin AH (2018) The challenges of natural fiber in manufacturing, material selection, and technology application: A review. J Reinf Plast Compos 37:770–779. https://doi.org/10.1177/0731684418756762

[3] Bourmaud A, Beaugrand J, Shah DU, et al (2018) Towards the design of high-performance plant fibre composites. Prog Mater Sci 97:347–408. https://doi.org/10.1016/j.pmatsci.2018.05.005

[4] Abtew MA Boussu F, Bruniaux P, et al (2019) Ballistic impact mechanisms – A review on textiles and fibre-reinforced composites impact responses. Compos Struct 223:110966. https://doi.org/10.1016/j.compstruct.2019.110966

[5] Comas-Cardona S, Le Grognec P, Binetruy C, Krawczak P (2007) Unidirectional compression of fibre reinforcements. Part 1: A non-linear elastic-plastic behaviour. Compos Sci Technol 67:507–514. https://doi.org/10.1016/j.compscitech.2006.08.017

[6] Hertz H, Jones DE, Schott GA (1896) On the contact of rigid elastic solids and on hardness. In: Miscellaneous Papers. Macmillan, pp 163–183

[7] M'Ewen E (1949) XLI. Stresses in elastic cylinders in contact along a generatrix (including the effect of tangential friction). London, Edinburgh, Dublin Philos Mag J Sci 40:454–459. https://doi.org/10.1080/14786444908521733

[8] Hadley D., Ward I., Ward J (1965) The transverse compression of anisotropic fibre monofilaments. Proc R Soc London Ser A Math Phys Sci 285:275–286. https://doi.org/10.1098/rspa.1965.0103

[9] Morris S (1968) 39—The Determination of the Lateral-Compression Modulus of Fibres. J Text Inst 59:536–547. https://doi.org/10.1080/00405006808660016

[10] Phoenix S, Skelton J (1974) Transverse Compressive Moduli and Yield Behavior of Some Orthotropic, High-Modulus Filaments. Text Res J 934–940. https://doi.org/doi:10.1177/004051757404401203

[11] Jawad SA, Ward IM (1978) The transverse compression of oriented nylon and polyethylene extrudates. J Mater Sci 13:1381–1387. https://doi.org/10.1007/BF00553190

[12] Cheng M, Chen W, Weerasooriya T (2004) Experimental investigation of the transverse mechanical properties of a single Kevlar® KM2 fiber. Int J Solids Struct 41:6215–6232. https://doi.org/10.1016/j.ijsolstr.2004.05.016

[13] Jones MCG, Lara-Curzio E, Kopper A, Martin DC (1997) The lateral deformation of cross-linkable PPXTA fibres. J Mater Sci 32:2855–2871. https://doi.org/10.1023/A:1018672400459

[14] Guo Z, Casem D, Hudspeth M, et al (2016) Transverse compression of two high-performance ballistic fibers. Text Res J 86:502–511. https://doi.org/10.1177/0040517515592814

[15] Sockalingam S, Bremble R, Gillespie JW, Keefe M (2016) Transverse compression behavior of Kevlar KM2 single fiber. Compos Part A Appl Sci Manuf 81:271–281. https://doi.org/10.1016/j.compositesa.2015.11.032

[16] Naito K, Tanaka Y, Yang JM (2017) Transverse compressive properties of polyacrylonitrile (PAN)-based and pitch-based single carbon fibers. Carbon N Y 118:168–183. https://doi.org/10.1016/j.carbon.2017.03.031

[17] Wollbrett-Blitz J, Joannès S, Bruant R, et al (2016) Multiaxial mechanical behavior of aramid fibers and identification of skin/core structure from single fiber transverse compression testing. J Polym Sci Part B Polym Phys 54:374–384. https://doi.org/10.1002/polb.23763

[18] Govilas J, Guicheret-Retel V, Amiot F, et al (2022) Platen parallelism significance and control in single fiber transverse compression tests. Compos Part A Appl Sci Manuf 159:106990. https://doi.org/10.1016/j.compositesa.2022.106990

[19] Gradshteyn I.S. and Ryzhik I.M. Table of integrals, series and products, seventh edition, Academic Press, 2007.

[20] SITARIST : Single fIber TrAnsverse compRessIon teSt with Tilt. https://doi.org/10.5281/zenodo.8301403